

## FEASIBILITY OF MATERIALS FOR ULTRAFILTRATION SYSTEM IN A SCWR

Gaelle Dupouy<sup>1</sup>, Peter E. Schalm<sup>1</sup>, Pascal Mertins<sup>1</sup>, Ian S. Butler<sup>2</sup>, Dominic H. Ryan<sup>3</sup>, Sikun G. Xu<sup>4</sup>, Janusz A. Kozinski<sup>5</sup>

<sup>1</sup> College of Engineering, University of Saskatchewan, Saskatoon,  
Saskatchewan, Canada S7N 5A9; [gad707@mail.usask.ca](mailto:gad707@mail.usask.ca)

<sup>2</sup> Department of Chemistry, McGill University, Montreal, Quebec, Canada H3A 2K6

<sup>3</sup> Department of Physics, McGill University, Montreal, Quebec, Canada H3A 2T8

<sup>4</sup> Chalk River Laboratories, AECL, Chalk River, Ontario, Canada K0J 1J0

<sup>5</sup> Faculty of Science and Engineering, York University, Toronto, Ontario, Canada M3J 1P3

### Abstract

One of the most important features in future SCWRs will be the coolant purification system, which removes impurities, particles, and radioactive materials as well as aids in the control of water chemistry. Several different options have been explored as ways to provide the high temperature and pressure purification that may be required. Different filter materials (stainless steel, chromium oxide, Ni-based alloys) have been tested in a dead-end configuration. This paper describes the preliminary results with SS316L ultrafiltration membranes. The mechanical integrity and particle removal efficiency of these different materials were examined and the results are presented here.

**Keywords:** Materials, Chemistry, Corrosion, Supercritical Water, Filtration, Purification

### 1. Introduction

The current worldwide nuclear power renaissance has resulted in a quest to develop a new generation of nuclear reactors (GEN IV) that are cheaper, safer, more efficient, and more resistant to proliferation. One of the proposed designs uses water in the supercritical state as the coolant, and is called the Supercritical Water Reactor (SCWR). This reactor would have a single phase (supercritical water) in the coolant loop with temperatures between 285-625°C and a pressure of 25.0 MPa as opposed to the two phases, water and steam, present in Boiling Water Reactors (BWRs) and Pressurized Light Water or Heavy Water Reactors (PWRs, PHWRs - notably CANDU<sup>®</sup> reactors). The proposed SCWR employs a direct SCW cycle for transporting heat and driving turbines for the generation of electricity.

The detailed water chemistry parameters for maintaining the integrity of the reactor materials and reactor safety have yet to be specified under the above conditions. As expected, the characteristics of soluble and insoluble corrosion products resulting from interactions between the coolant and the reactor equipment are not available. The lack of water chemistry reference and corrosion product characteristics could make it more challenging to develop purification systems that effectively control the required chemical parameters. The removal of particulates and ionic species (impurities, particles, and radioactive materials) to maintain optimized chemistry parameters of the coolant is an essential part of control protocols for operating a nuclear power reactor.

Currently, most reactor coolant purification systems use liquid cartridge filters and ion-exchange resins working at temperatures around 50~60 °C for the heat transport system (HTS) or

simply by boiler blow-down water for the secondary side of steam generators. There is an expectation that low-temperature purification might not be efficient enough to meet the purification challenges such as preventing radioactivity from being transported to other interfacing equipment in a single phase, direct cycle SCW system. The use of ion-exchange resins is also expected to generate large volumes of spent resin because corrosion products have a higher solubility at sub-critical conditions than in SCW. In addition, energy loss is inevitable during the process of lowering the coolant to a 50-60 °C operating temperature.

Thus, there is a need to determine the feasibility of developing a high temperature-pressure purification system for SCWR operation. Supercritical water presents a host of challenges to purification system designers because of its extremely high temperature, low solubility of inorganic materials, lack of high density liquid phase to entrain particles, and its ability to dissolve radioactive gases. Several different methods have been proposed as ways to provide the high temperature and pressure purification needed. These methods include both metal and ceramic membranes, stainless-steel supported ceramic membranes, stainless-steel hydro cyclones, and nozzle SCW techniques.<sup>[1-4]</sup> For example, Goemans has used a cross flow micro-filter made of austenitic stainless steel SS316L and has achieved good results at 455°C.<sup>[5]</sup> However, SS316L may not be useful at the high temperatures expected in a SCWR due to the high level of corrosion in these anticipated conditions.<sup>[6]</sup> The objective of this project is to find an effective system for filtration at high temperature and pressure.

New systems need to be designed with new materials. Some recent publications show the corrosion properties of candidate materials.<sup>[6-12]</sup> Based on these results, we decided to test materials with a high corrosion resistance and compare the results with a common and cheaper material, SS316L. In the first phase, several materials are tested in a dead-end configuration. This method is used for several reasons: the cost is cheaper, the system is simpler, and it is easier to characterize the material both before and after the experiment. The second phase is to develop and optimize a practical method for SCW filtration.

## 2. Experiment

### 2.1. Apparatus

Figure 1 shows a schematic diagram of the experimental apparatus used in this study. This system consists of a high-pressure pump (Gilson 305 HPLC pump), a preheater (two cable heater, Watlom), an electric furnace (3210 split tube furnace, 18" long., ATS), the test membrane, a heat exchanger, an in-line filter, and a back pressure regulator (Tescom). The connectors and the tubing are made of SS316L (Swagelok) with a ¼" OD.

This system is designed to simulate a SCWR. The HPLC pump injects water into the system, the preheater mimics the nuclear reactor core, the furnace recreates the environment in the tubing between the reactor core and turbine, and the heat exchanger replaces the turbine. For the moment, the system is not a closed cycle so that the final solution can be characterized. The test membrane rests at the end of the furnace. The membrane has an outer diameter of ¼" and a thickness of about 0.062". A pressure drop of 0.2 MPa can be observed between P1 and P2, where P1 is always higher than P2.

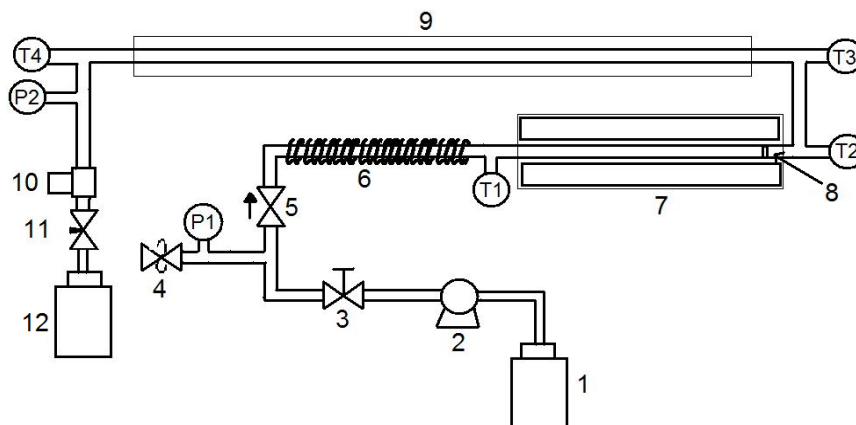


Figure 1. Schematic diagram of the experimental apparatus. (1) feedstock of aqueous  $\text{Al}(\text{NO}_3)_3$  solution; (2) high-pressure pump; (3) valve; (4) relief valve; (5) check valve; (6) preheater; (7) electric furnace; (8) membrane; (9) heat exchanger; (10) in-line filter; (11) back-pressure regulator; (12) reservoir.

## 2.2. Procedure

Initially, metal oxides were injected into the system to simulate the corrosion products expected in a SCWR. This method did not work because the oxides are insoluble in water and did not move due to the weak flow rate so the particles stuck to the walls of the tubing. Thus, metal salts were used instead of oxides and led to precipitates of metal oxides in order to simulate particulate corrosion products expected in a SCWR.

Aluminum nitrate (salt) is used because its reaction in supercritical water has already been studied.<sup>[13-17]</sup> The aluminum cation was chosen because this ion is not present in the system materials (SS316L), so the true efficiency of the filter can be characterized. In addition, aluminum oxides are white which allows us to see the presence of the corrosion product. Nitrate salt was chosen over chloride or bromide salts because it is less oxidizing than either chloride or bromide, making it ideal for a SCWR. Moreover, nitrate salt was used in almost all publications about the syntheses of oxide particles in supercritical water, and no problems of corrosion have been reported.<sup>[13, 14, 16-18]</sup>

The aluminum nitrate solution was injected into the system (after pressurization to 25 MPa at ambient temperature) at a flow rate of  $2 \text{ g}\cdot\text{min}^{-1}$ . The solution was heated above the critical point in the preheater and the aluminum was precipitated as  $\text{AlOOH}$  and  $\text{Al}_2\text{O}_3$  particles.<sup>[14, 15, 19]</sup> The aluminum oxide particles then passed through the furnace where the temperature was stabilized at  $550^\circ\text{C}$ . The temperatures of the preheater and the furnace were monitored by K-type thermocouples and controlled by a Variac controller. The test membrane (inside the furnace) collected the particles and the remainder of the solution continued through the heat exchanger and was collected in a reservoir. An in-line filter of  $2\text{-}\mu\text{m}$  pore size was used to protect the back pressure regulator in case the membrane was destroyed. The pore size was large enough that it did not block any particles that bypass the test membrane, and therefore should not affect our data. The system pressure was set using a back pressure regulator at the exit of the system. The fluctuation of the system pressure was around 0.2 MPa due to the pump. In the future, a new pump will be used (Lab Alliance Prep24) to reduce the fluctuation to 0.05 MPa. All of the parameters (pressure and temperature) were collected with an Omega-4718 module.

## 2.3. Analyses

The concentration of aluminum, iron, and chromium atoms in the final solution was determined by Inductively Coupled Plasma Mass Spectrometry analysis (Perkin Elmer Elan 5000 ICP-MS). We assume that at 550°C all the aluminum atoms were precipitated.<sup>[15, 19]</sup> So, the ICP data showed the quantity of aluminum oxides not captured by the membrane. Iron and chromium concentrations were measured to observe the natural corrosion of the system.

The membrane was dried in an oven and then weighed, both before and after the experiment, in order to measure the weight loss or gain due to corrosion and oxide layer deposition. The first visual characterization used a microscope with a camera to take pictures. The membrane and the powder were characterized by powder X-ray diffraction (XRD) (Rigaku D/MAX-B with Co K $\alpha$  radiation).

Finally, the membrane and the powder layer were observed using a Scanning Electron Microscope (SEM) (Philips 505). The non-metallic samples (powder and ceramic membrane) had to be gold coated to increase electrical conductivity and reduce charging effects.

## 3. Results

### 3.1. Size and morphology of aluminum oxide particles.

After experiments when aluminum nitrate was injected, a layer of white powder was observed on the membrane. Figure 2a shows a photograph of the powder. The SEM pictures (Figure 2b) show different morphologies of the particles. The size distribution of the powder is between 0.1  $\mu\text{m}$  and 20  $\mu\text{m}$ , the same size expected to be found in the SCWR.<sup>[20-22]</sup> The characterization by XRD (Figure 3) shows peaks of AlOOH and  $\alpha\text{-Al}_2\text{O}_3$  oxides.<sup>[14, 15, 23]</sup>

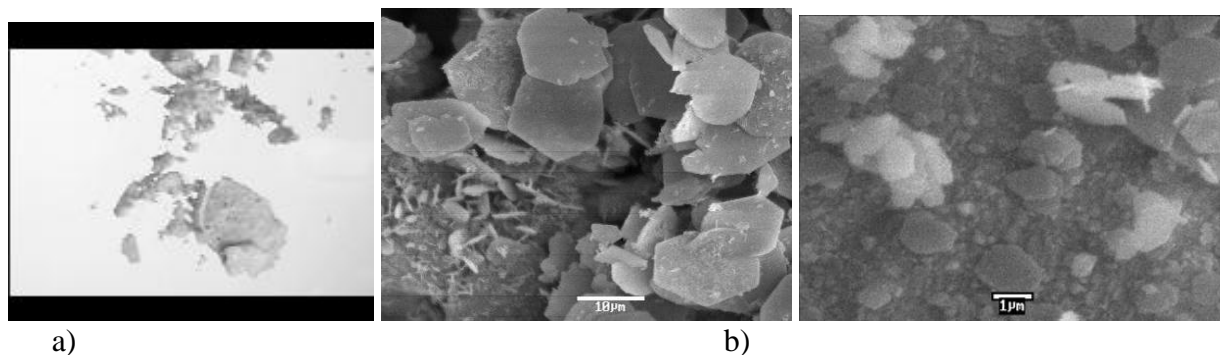


Figure 2. Pictures of the white powder obtained after injection of aluminum nitrate, a) by microscope and b) by SEM.

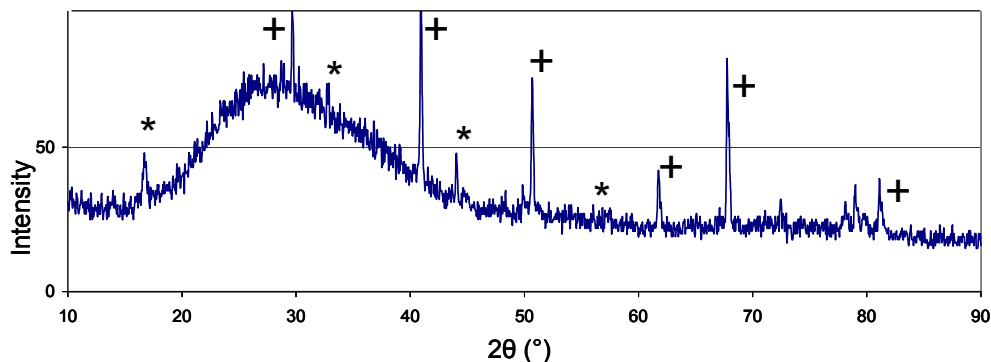


Figure 3. Diffractograms of the white powder. (\*) for AlOOH and (+) for  $\alpha$ -Al<sub>2</sub>O<sub>3</sub>.

### 3.2. Austenitic stainless steel SS316L

The first phase of this project was to test a common and inexpensive material, the austenitic stainless steel SS316L. The membrane filters were from Mott Corporation. Each filter was pressed separately for consistent size and porosity. The average pore size was 0.2  $\mu$ m and the initial weight varied from 315.3 to 317.8 mg.

Several pictures of the membranes are shown in Figure 4. Picture 4a shows an unused membrane. Picture 4b shows a membrane used for 2h without the injection of aluminum nitrate, and 4c a membrane used for 2h with injection of aluminum nitrate. The corrosion of the material (Figure 4b) can be seen with the naked eye indicating a strong oxidation by the supercritical water. The powder layer on the used membrane (Figure 4c) is white and contains different metal oxides. Between the white powder and the membrane, an orange layer can be seen (d). This layer is due to the corrosion of the membrane by the supercritical water (see Figure 4b).

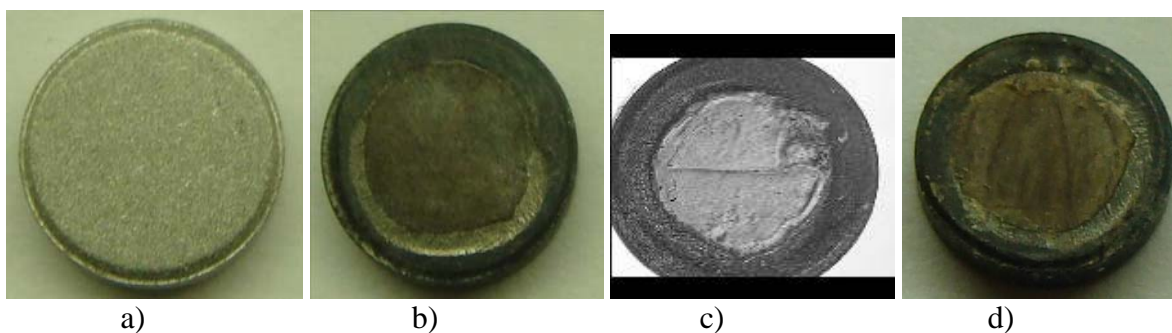


Figure 4. Pictures by camera of a) unused membrane, b) used membrane without injection of nitrate, c) used membrane with injection of nitrate and d) membrane c with powder removed.

SEM pictures of the membranes after nitrate injection are shown in Figure 5. The surface of the membrane is not uniform and the holes near the surface are bigger than 0.2  $\mu$ m. These pictures show that a lot of powder is deposited on the surface of the membrane.

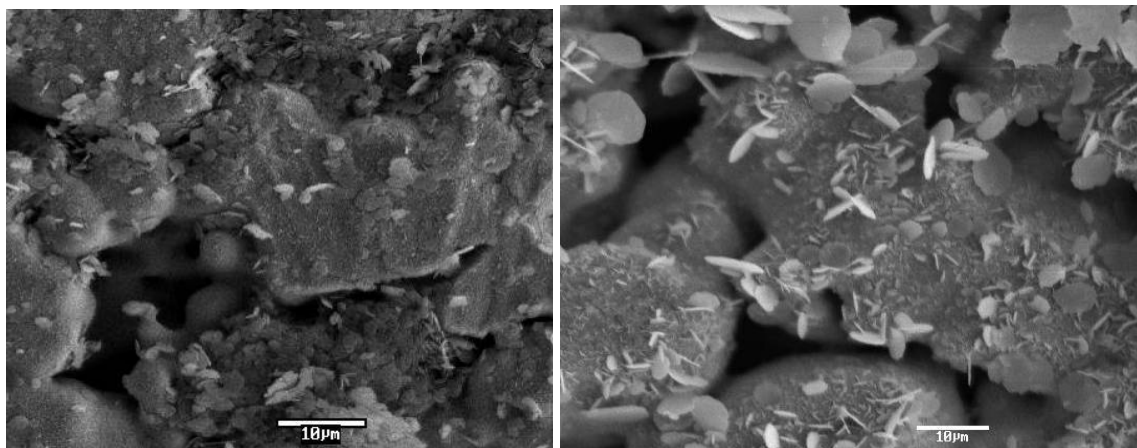


Figure 5. SEM pictures of the surface of used membranes after injection of aluminum nitrate.

The characterization by XRD is shown in Figure 6. SS316L (a) shows three peaks between 10 and 90° which represent the  $\alpha$  Fe structure. The used membrane (b) shows the same peaks along with very small peaks at different values. The membrane (c) shows several peaks, which represent the combination of the used membrane, (b), and the white powder (d) which contains different aluminum oxides.

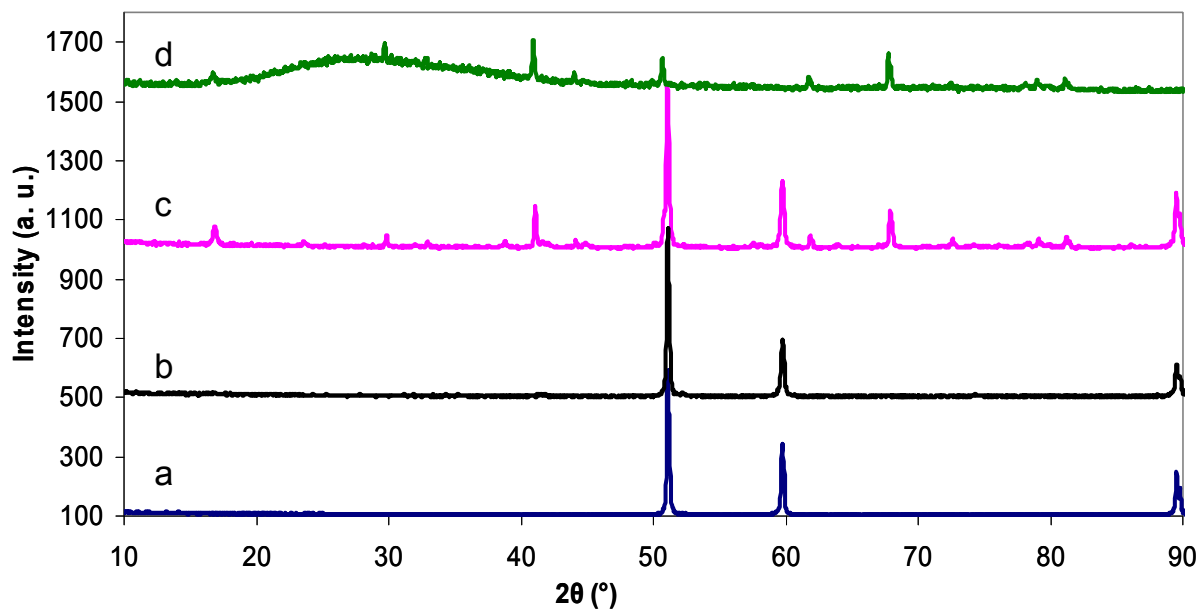


Figure 6. Diffractograms of a) unused membrane, b) used membrane without injection of aluminum nitrate, c) used membrane with injection of aluminum nitrate, d) white powder on membrane with injection of aluminum nitrate.

During the experiments, a trans-membrane pressure drop occurred due to the formation of the oxide layer (cake) on the surface of the filter. The pressure after the membrane (P2) was stable at 25 MPa (controlled by the back pressure regulator) and the pressure before, P1, varied between 25 and 27 MPa (depending to the duration of the experiment and the concentration of the aluminum nitrate

injected). Regardless of pressure fluctuations, the water in the system remained supercritical so its properties did not change significantly.

Upon weighing the membrane, a mass gain due to corrosion could be observed as well as the formation of an oxide layer. The experimental conditions were 550°C and 25 MPa with an injection time of 2h. In experiments without injection of aluminum nitrate, the weight of the membrane increased by about 3 mg (1 %) due to the oxidation of the surface. In experiments with injection of aluminum nitrate, the weight of the membrane increased by around 6 mg (2 %) due to corrosion and the powder layer, thus the aluminum oxide layer contributed around 3 mg (Table 1).

Exp #	Membrane weight (mg)			Element weight (mg)					Efficiency (%)
	Before	After	$\Delta w$	Al injected	Final solution			Al captured	
					Al	Cr	Fe		
1	316.2	323.0	6.8	1.031	0.091	0.077	0	0.940	91.2
2	316.3	321.9	5.6	1.126	0.162	0.115	0.004	0.964	85.6
3	315.9	321.7	5.8	1.108	0.059	0.132	0	1.049	94.7
4	315.4	320.6	5.2	1.100	0.109	0.106	0	0.991	90.0
5	315.5	321.6	6.1	1.145	0.075	0.152	0	1.070	93.4

Table 1. Results of membrane weighing and ICP measurements.

ICP results are shown in Table 1. The experimental conditions were 550°C and 25 MPa with an injection time of 2h. The data show that the mass of aluminum ions captured by the membrane was around 1 mg in all of experiments. Based on the XRD results, we consider that aluminum nitrate was precipitated in a mixture of AlOOH and Al<sub>2</sub>O<sub>3</sub>. The weight ratio of M(AlOOH)/M(Al) and M(Al<sub>2</sub>O<sub>3</sub>)/M(Al) are 2.22 and 3.78, respectively. Thus, the mass of the captured aluminum can be multiplied by 3 to get an average value of the mass of aluminum oxides stuck on the membrane. In these experiments, the average mass of aluminum ions captured by the membrane is 1mg which agrees with an observed mass increase of 3 mg due to the oxide layer.

We calculate that the SS316L membrane removes between 85 and 95% of aluminum oxide particles, which is a good standard with which to compare future results. It appears that some chromium is released from the system materials when heating is stopped, likely during the transition from supercritical to subcritical conditions.

#### 4. Conclusion and Future Steps

Our results demonstrate that SS316L is an efficient filter, but this material is not good for the high temperatures employed due to the high degree of corrosion. Regarding the system, SS316L has a recommended temperature limit of 537°C, so tubing of Alloy 625 will replace those of SS316L for the preheater and the furnace. New membranes made of Ni-Alloy (Alloy C-276 and Alloy 625) will be tested in future work. Moreover, some studies will be conducted on ceramic and ceramic/metal filters.

#### 5. Acknowledgements

The authors gratefully acknowledge the NSERC/NRCan/AECL Gen IV Energy Technologies Program for financial support of this research.

## 6. References

- [1] P. C. Dellorco, L. Li, and E. F. Gloyna, "The Separation of Particulates from Supercritical Water Oxidation Processes", *Separation Science and Technology*, Vol. 28, 1993, pp. 625-642.
- [2] L. X. Li, and E. F. Gloyna, "Separation of ionic species under supercritical water conditions", *Separation Science and Technology*, Vol. 34, 1999, pp. 1463-1477.
- [3] H. Y. Gao, Y. D. Li, J. Y. S. Lin, and B. Q. Zhang, "Characterization of zirconia modified porous stainless steel supports for Pd membranes", *Journal of Porous Materials*, Vol. 13, 2006, pp. 419-426.
- [4] J. A. Kozinski, I. Butler, D. H. Ryan, and S. G. Xu, "Application of high-temperature/pressure phase separation to a supercritical water cooled reactor", *ISSCWR4*, Vol., 2009, pp.
- [5] M. G. E. Goemans, F. M. Tiller, L. X. Li, and E. F. Gloyna, "Separation of metal oxides from supercritical water by crossflow microfiltration", *J. Membr. Sci.*, Vol. 124, 1997, pp. 129-145.
- [6] S. Penttila, A. Toivonen, L. Heikinheimo, and R. Novotny, "Corrosion Studies of Candidate Materials for European Hplwr", *Nuclear Technology*, Vol. 170, 2010, pp. 261-271.
- [7] P. Kritzer, "Corrosion in high-temperature and supercritical water and aqueous solutions: a review", *Journal of Supercritical Fluids*, Vol. 29, 2004, pp. 1-29.
- [8] R. L. Klueh, and A. T. Nelson, "Ferritic/martensitic steels for next-generation reactors", *Journal of Nuclear Materials*, Vol. 371, 2007, pp. 37-52.
- [9] C. W. Sun, R. Hui, W. Qu, and S. Yick, "Progress in corrosion resistant materials for supercritical water reactors", *Corrosion Science*, Vol. 51, 2009, pp. 2508-2523.
- [10] Y. Nakazono, T. Iwai, and H. Abe, *Journal of Physics: conference series*, Vol. 215, 2010, pp. 012094.
- [11] H. Kim, D. B. Mitton, and R. M. Latanision, "Corrosion behavior of Ni-base alloys in aqueous HCl solution of pH 2 at high temperature and pressure", *Corrosion Science*, Vol. 52, 2010, pp. 801-809.
- [12] H. Kim, D. B. Mitton, and R. M. Latanision, "Effect of pH and Temperature on Corrosion of Nickel-Base Alloys in High Temperature and Pressure Aqueous Solutions", *Journal of the Electrochemical Society*, Vol. 157, 2010, pp. C194-C199.
- [13] T. Adschiri, K. Kanazawa, and K. Arai, "Rapid and Continuous Hydrothermal Synthesis of Boehmite Particles in Subcritical and Supercritical Water", *Journal of the American Ceramic Society*, Vol. 75, 1992, pp. 2615-2618.
- [14] Y. Hakuta, H. Ura, H. Hayashi, and K. Arai, "Effects of hydrothermal synthetic conditions on the particle size of gamma-AlO(OH) in sub and supercritical water using a flow reaction system", *Materials Chemistry and Physics*, Vol. 93, 2005, pp. 466-472.
- [15] T. Noguchi, K. Matsui, N. M. Islam, Y. Hakuta, and H. Hayashi, "Rapid synthesis of gamma-Al<sub>2</sub>O<sub>3</sub> nanoparticles in supercritical water by continuous hydrothermal flow reaction system", *Journal of Supercritical Fluids*, Vol. 46, 2008, pp. 129-136.
- [16] N. Lock, P. Hald, M. Christensen, H. Birkedal, and B. B. Iversen, "Continuous flow supercritical water synthesis and crystallographic characterization of anisotropic boehmite nanoparticles", *Journal of Applied Crystallography*, Vol. 43, 2010, pp. 858-866.
- [17] M. T. Liang, S. H. Wang, Y. L. Chang, H. I. Hsiang, H. J. Huang, M. H. Tsai, W. C. Juan, and S. F. Lu, "Iron oxide synthesis using a continuous hydrothermal and solvothermal system", *Ceramics International*, Vol. 36, 2010, pp. 1131-1135.
- [18] Y. L. Hao, and A. S. Teja, "Continuous hydrothermal crystallization of alpha-Fe<sub>2</sub>O<sub>3</sub> and Co<sub>3</sub>O<sub>4</sub> nanoparticles", *Journal of Materials Research*, Vol. 18, 2003, pp. 415-422.

- [19] N. Lock, M. Bremholm, M. Christensen, J. Almer, Y. S. Chen, and B. B. Iversen, "In Situ High-Energy Synchrotron Radiation Study of Boehmite Formation, Growth, and Phase Transformation to Alumina in Sub- and Supercritical Water", *Chemistry-a European Journal*, Vol. 15, 2009, pp. 13381-13390.
- [20] M. Bolz, W. Hoffmann, W. Rühle, and F. Becker, Characterization of colloids in primary coolant, in *Water Chemistry of Nuclear Reactor Systems 7*, Vol 1, 1996, pp. 42-46.
- [21] J. Brunning, P. Cake, B. Bengtsson, G. Granath, and J. Kvint, Corrosion product measurements at Ringhals 1, in *Water Chemistry of Nuclear Reactor Systems 7*, Vol 1, 1996, pp. 103-105.
- [22] J. Brunning, P. Cake, A. Harper, and P. K. Tait, Assessment of reactor primary coolant sampling data under steady full power operation, in *Water Chemistry of Nuclear Reactor Systems 7*, Vol 1, 1996, pp. 54-61.
- [23] Y. Wang, and W. J. Thomson, "Characterization of the spinel phase in a diphasic mullite gel using dynamic X-ray diffraction", *Journal of Materials Science*, Vol. 34, 1999, pp. 3577-3580.